American Mineralogist, Volume 83, pages 373–382, 1998

Relationships between microstructure and composition in enargite and luzonite

MIHÁLY PÓSFAI* AND PETER R. BUSECK

Department of Geology and Chemistry, Arizona State University, Tempe, Arizona 85287-1404, U.S.A.

ABSTRACT

$Cu_3(As,Sb)S_4$ minerals commonly contain structurally disordered crystals of intergrown enargite and the luzonite-famatinite series (Pósfai and Sundberg 1998). Here we discuss the relationships between the fine-scale structural variations and the Sb/As ratios of these minerals. Although luzonite typically contains more Sb than enargite, individual layers of luzonite within Sb-bearing enargite are not associated with higher Sb/As ratios. Defect-free enargite can also contain Sb. We develop a ''structure-composition'' diagram in which both the structural enargite-luzonite and the compositional luzonite-famatinite solid solutions can be represented. Compositions plotted in this diagram reveal that Sb-bearing enargite and luzonite contain only a relatively small number of defects, whereas Sb-free crystals can be heavily disordered. Coexisting enargite and famatinite and zoning in luzonite-famatinite indicate fluctuations in the Sb-content of the fluid during ore deposition. On the other hand, assemblages of Sb-free enargite and luzonite probably reflect thermal oscillations; heavily disordered, intermediate structures may have formed near the transition temperature of low-temperature luzonite to high-temperature enargite. Our results suggest that characteristic microstructures in enargite, luzonite, and famatinite can be useful for constraining fluid composition and temperature during ore deposition.

INTRODUCTION

In a companion study (Pósfai and Sundberg 1998) we show that enargite and luzonite are intergrown on the atomic scale. Some crystals are defect-free, whereas others contain disordered stacking sequences of close-packed layers. The correlation, if any, between the fine-scale structures and compositional variations is not known. Because such features also occur in other mineral groups, the problem is of general interest.

Minerals with compositions of $Cu_3(As,Sb)S_4$ include enargite, luzonite, and famatinite. Enargite has an orthorhombic, hexagonal close-packed (hcp) structure, whereas luzonite and famatinite are the two end-members of the tetragonal, cubic close-packed (ccp) solid-solution series between Cu_3AsS_4 and Cu_3SbS_4, respectively (Fleischer and Mandarino 1995). Because enargite and luzonite differ only in the stacking sequence of structurally and compositionally identical layers, they can be regarded as polytypes.

Wet chemical and microprobe analyses of $Cu_3(As,Sb)S_4$ minerals (Gaines 1957; Lévy 1967; Springer 1969; Sugaki et al. 1976) show that a continuous solid-solution series exists between luzonite (Cu_3AsS_4) and famatinite (Cu_3SbS_4). When enargite and luzonite coexist, the latter generally contains more Sb; for enargite, the most Sb-rich composition was found to be $Cu_3As_{0.8}Sb_{0.2}S_4$ (Gaines 1957; Springer 1969).

Phase relationships between enargite and the luzonite-famatinite series above 350 °C were established by studies of the Cu-As-S (Skinner 1960; Maske and Skinner 1971), Cu-Sb-S (Skinner et al. 1972), and Cu-As-Sb-S (Feiss 1974; Luce et al. 1977; Kanazawa 1984; Sugaki et al. 1982) systems; however, phase relations below ~350 °C remain largely unknown. Luce et al. (1977) and Sugaki et al. (1982) emphasized the difficulties of obtaining structurally and chemically homogeneous phases below 400 °C. According to Skinner (1960), luzonite is the low-temperature form of Cu_3AsS_4; the inversion temperature is estimated to lie between 280 and 300 °C (Maske and Skinner 1971) (Fig. 1). These studies indicate that above ~280 °C and on the micrometer scale (as determined by optical microscopy) the formation of either enargite or luzonite-famatinite is determined by the Sb/As ratio of the fluid (Fig. 1). It is not clear, however, whether the Sb content controls the formation of disordered crystals that are structurally intermediate between enargite and the luzonite-famatinite series (Pósfai and Sundberg 1998).

The use of high-resolution transmission electron microscopy (HRTEM) in combination with selected-area electron diffraction (SAED) and energy-dispersive X-ray spectrometry (EDS) offers an opportunity to study structural and compositional features in enargite and luzonite at a much finer scale than was possible with other methods. We studied interfaces at high resolution and determined the average structures and compositions of disordered crystals; by doing this, we wished to establish a link between results that can be obtained at the different

* Permanent address: Department of Earth and Environmental Sciences, University of Veszprém, Veszprém POB 158, H-8201 Hungary.

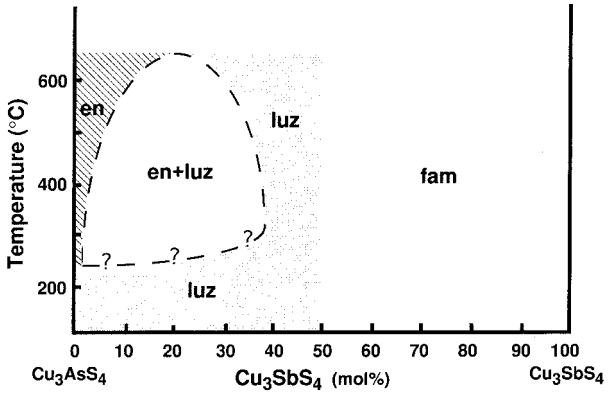

FIGURE 1. Temperature-composition diagram of the Cu_3AsS_4-Cu_3SbS_4 join (en = enargite; luz = luzonite; fam = famatinite). After Barton and Skinner (1967) and Feiss (1974), and modified on the basis of data by Maske and Skinner (1971) and Sugaki et al. (1982).

levels of resolution that are available using optical or microprobe and HRTEM methods. Our primary goal was to reveal whether on a much smaller scale, as far down as individual close-packed layers, the formation of distinct structural units (such as stacking defects) is controlled by composition. The occurrence of two polytypes in the same sample and the formation of heavily disordered crystals are problems of broad mineralogical interest; the results obtained from enargite and luzonite can be useful for solving such problems.

EXPERIMENTAL METHODS

We studied the same samples described by Pósfai and Sundberg (1997). Ion-milled specimens were prepared from enargite and luzonite individually and from boundary regions between them. Pieces were ground to fit into a 2 mm long, 0.5 mm wide slot in a 3 mm diameter Al disk. Samples were glued into the slot with epoxy,

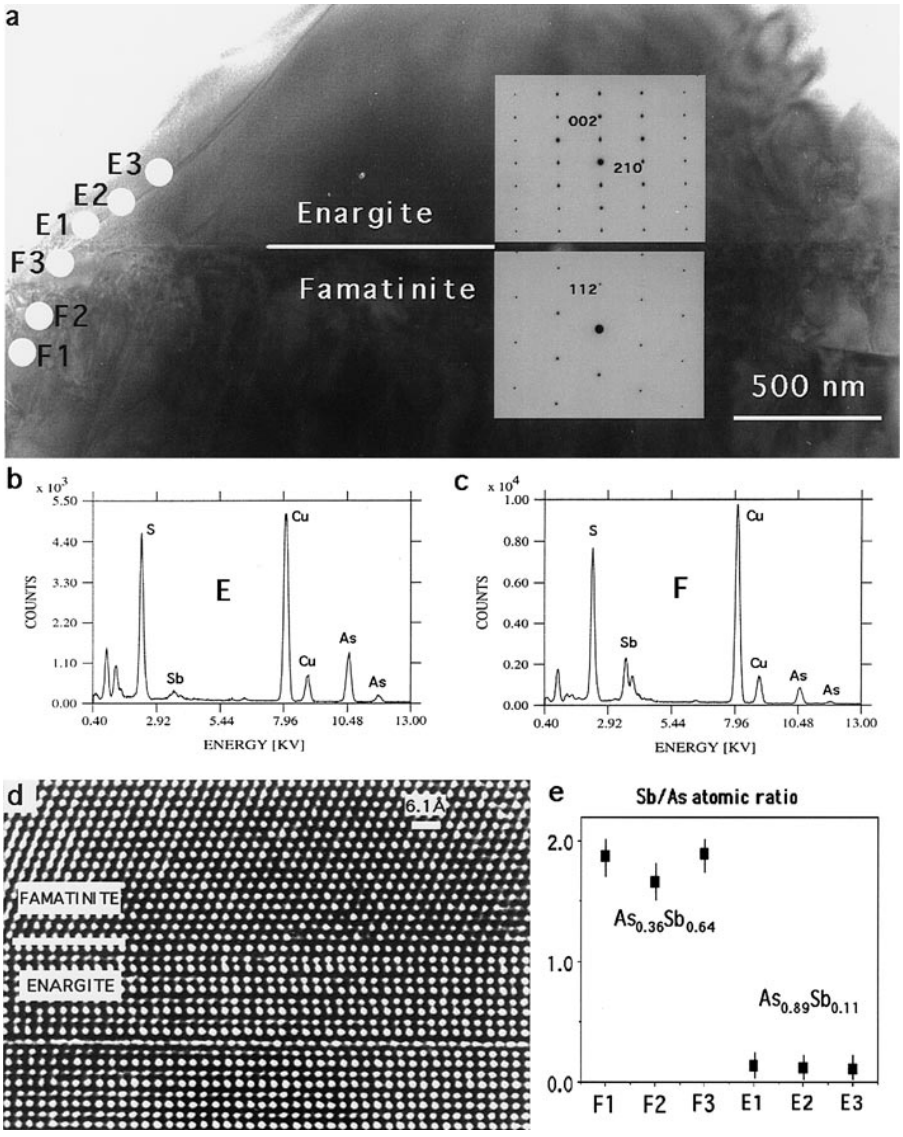

FIGURE 2. (**a**) Low-magnification image of a coherent intergrowth of enargite and famatinite with corresponding SAED patterns; typical EDS spectra obtained from (**b**) enargite and (**c**) famatinite; (**d**) high-resolution image of the interface; and (**e**) Sb/As atomic ratios obtained from the areas marked by white spots in (**a**).

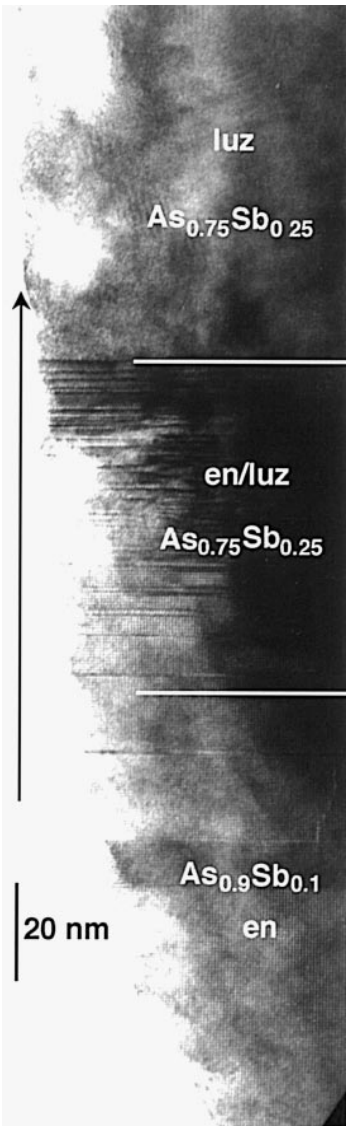

FIGURE 3. Intergrowth of enargite and luzonite. The atoms per formula unit are shown for As and Sb for both phases. A structurally disordered zone is marked ''en/luz.'' The arrow shows the assumed direction of crystal growth (see Discussion).

ground, and ion-milled. The slotted Al supports were used to avoid the contribution of X-rays from the Cu grids in EDS spectra and to maximize the area useful for TEM studies. We also studied crushed specimens to detect potential changes caused by ion milling.

Most results presented here were obtained from five ion-milled samples that were prepared from one hand specimen of enargite ore. We also studied ion-milled and crushed TEM samples from other hand specimens from the Recsk mine and from Mankayan (Philippines), Quiruvilca (Peru), and Cosihuiriachic (Mexico). All showed features similar to those from Recsk.

All SAED patterns and electron micrographs here are from crystals that were aligned with their close-packed

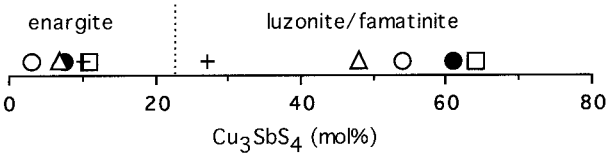

FIGURE 4. Cu_3SbS_4 content in intergrown enargite and luzonite-famatinite crystals, obtained from EDS analyses. The estimated error of measurement is ±3 mol% Cu_3SbS_4. Identical symbols indicate pairs of enargite and luzonite-famatinite crystals on opposite sides of interfaces. The dotted line separates the hcp and ccp structures.

layers parallel to the electron beam. For high-resolution imaging we used a JEOL 4000EX microscope operated at 400 kV accelerating voltage (C_s = 1.0 mm), using a top-entry, double-tilt ($x,y = \pm 25°$) goniometer stage. Most analytical electron microscopy was done using a 200 kV, JEOL 2000FX electron microscope equipped with a Kevex X-ray detector. Spectra were processed and quantified using the Quantex program. K factors for Cu and As were experimentally determined from Sb-free enargite and for Sb from chalcostibite ($CuSbS_2$). For the EDS analyses of single faults, a 200 kV, Philips CM200

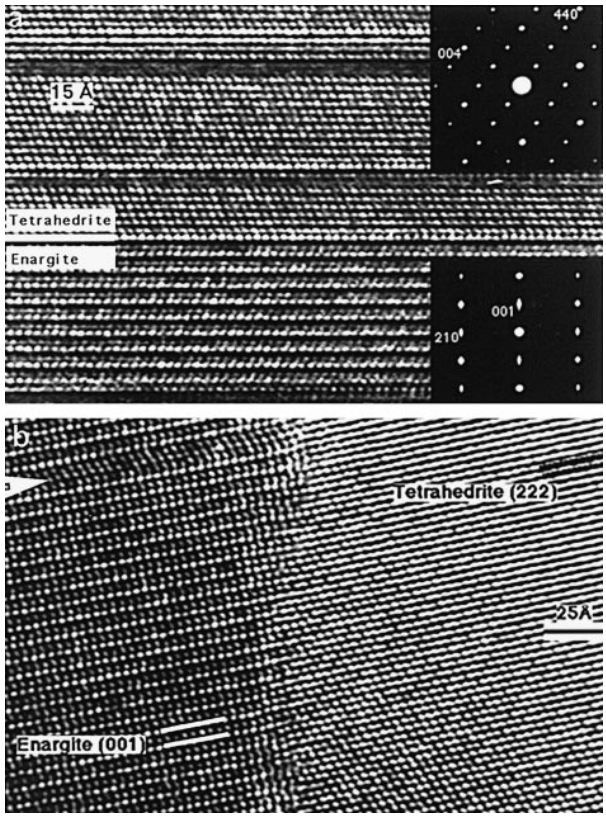

FIGURE 5. Intergrowths between enargite and Mn-bearing tetrahedrite. The interface is parallel to the close-packed layers in (**a**) and irregular in (**b**). The white arrow in (**b**) marks a stacking fault in enargite. Both images were obtained with the electron beam parallel to $[\bar{1}20]$ of enargite and $[\bar{1}10]$ of tetrahedrite.

FEG electron microscope was used that produces an electron beam that has a diameter as small as 2 nm. In many cases the same sample areas were studied with more than one instrument so that both high-resolution images and EDS spectra would be available.

RESULTS

Analyses of interfaces

Structural and chemical boundaries (enargite and luzonite-famatinite). We collected EDS spectra (at the white spots in Fig. 2a) near boundaries between enargite and luzonite-famatinite. For analyses E1 and F3, the electron beam was positioned as close to the boundary as possible while still keeping it within one phase. X-ray spectra of the two minerals (Figs. 2b and 2c) show large differences in the As and Sb peaks but are otherwise identical. The inserted SAED patterns in Figure 2a reveal that the two minerals are intergrown along their close-packed planes [(002) in enargite and (112) in famatinite]. The HRTEM image in Figure 2d and the Sb/As ratios (Fig. 2e) indicate an abrupt change at the boundary; neither a structurally nor a chemically intermediate region between enargite and famatinite is present. Apart from a few stacking faults, both minerals have ordered structures.

Another interface between enargite and luzonite (Fig. 3) shows a structurally disordered transition zone (marked ''en/luz'') that has the same composition as the luzonite. The sharp chemical boundary occurs approximately at the lower white line. The compositions of coexisting pairs of enargite and luzonite-famatinite crystals that were analyzed on opposite sides of interfaces (at increasing distances from the border) are plotted in Figure 4 (including data from the boundaries shown in Figures 2 and 3 and from three other interfaces). In all these intergrowths $(001)_{en}$ is parallel to $(112)_{luz}$.

Interfaces between enargite and Mn-bearing tetrahedrite occur in many places; because such boundaries are similar to those between enargite and luzonite, we discuss them here. Some are parallel to the close-packed planes of enargite and tetrahedrite (Fig. 5a). In other places the boundry is irregular (Fig. 5b), the close-packed (002) planes of enargite continue across the interface grading into the close-packed (222) planes of tetrahedrite. In both intergrowths an abrupt change occurs in the Sb/As ratio from low-Sb enargite to high-Sb tetrahedrite. The average formula of the tetrahedrite crystals is about $Cu_{10.4}Mn_{1.4}Sb_{2.3}As_{1.7}S_{13}$, which is within the compositional range of other natural (Basu et al. 1984) and synthetic (Makovicky and Karup-Møller 1994) Mn-bearing tetrahedrites.

Chemical boundaries without structural changes (zoned luzonite). Many crystals from Recsk that have the ccp luzonite-famatinite structure exhibit chemical zoning if they contain Sb. Compositions obtained along the edge of a large (~20 μm long) luzonite crystal show three zones that have markedly different Sb/As ratios (A, B, and C in Fig. 6) but identical SAED patterns. Zone boundaries could be detected primarily on the basis of EDS spectra; only a slight contrast change is evident in the electron micrographs, indicating that the structure does not change across the chemical boundaries. No gradual transition between low- and high-Sb zones can be observed when a 20 nm electron beam is used for the analyses; i.e., whereas the Sb/As ratio is almost constant within zones that are several micrometers thick, it can change by as much as 0.2 within as short a distance as about 20 nm (or possibly even less).

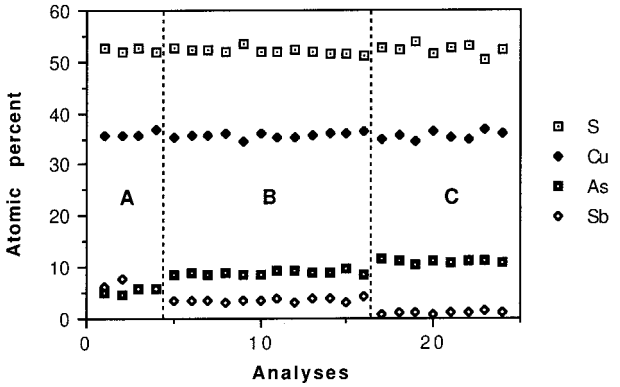

FIGURE 6. Compositions obtained from a zoned luzonite-famatinite crystal. A, B, and C mark three zones that differ in their Sb/As ratios.

The S/(Cu+As+Sb) ratios in Figure 6 are consistently higher than 1, the value for stoichiometric luzonite. In general, our EDS analyses indicate variable S/(Cu+As+Sb) ratios for both hcp and ccp crystals. Because such deviations from stoichiometric values depend strongly on the crystallographic orientation of the analyzed grain, we interpret them as resulting from channeling effects (for an explanation of electron channeling and its effect on analyses see Buseck and Self 1992). Sb and As atoms occupy the same crystallographic positions in both enargite and luzonite, thus their relative concentrations obtained from EDS spectra are unaffected by channeling.

Structural boundaries without chemical change (Sb-free enargite/luzonite). Crystals with strongly disordered stackings of close-packed layers occur in enargite and luzonite (Pósfai and Sundberg 1998). The SAED patterns in Figure 7 represent the large variety of structures that occur within an area several micrometers across. In Figure 7a the enargite reflections are broad; strong diffuse scattering connects them along [001]*. Based on a count of hcp and ccp layers in the corresponding high-resolution image (not shown here), the average structure of this crystal is about 70% enargite, 30% luzonite. The pattern in Figure 7b shows a luzonite crystal that is heavily disordered along one [112]*-type direction. The faint diffuse scattering along two sets of reciprocal lattice rows in Figure 7c indicates that this crystal has a low density of stacking faults along both (112)-type sets of close-packed planes that are seen edge-on in this orientation. An ordered luzonite crystal is shown in Figure 7d.

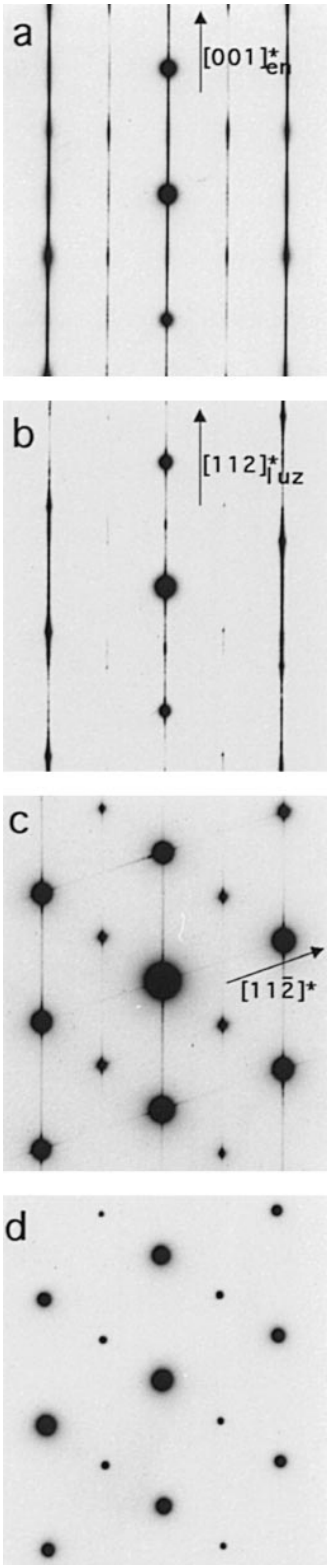

FIGURE 7. SAED patterns obtained from crystals within a few micrometers of one another. (**a**) strongly disordered enargite; (**b**) strongly disordered luzonite; (**c**) luzonite slightly disordered along two directions; (**d**) ordered luzonite.

Variations of the average structure are apparent in the low-magnification image of Figure 8. We can regard this area as consisting of five crystals, marked I, II, III, IV, and V. All have their [110] zone axis parallel to the electron beam, and most of their boundaries are stepped or straight twin planes. Because the angle between the two twin planes (112) and (11$\bar{2}$) is 72° in luzonite, the orientational relationships between the five crystals result in a fivefold symmetry of the ten 112-type reflections around 000; these ten reflections are marked by arrows in the inserted SAED pattern. Areas can be distinguished that have (A) almost fault-free luzonite structure; (B) slightly disordered luzonite structure with intersecting faults and twins; (C) a low density of stacking faults along one (112)-type plane; and (D) heavily disordered structures along one direction. In some crystals, sharp boundaries occur between ordered luzonite and heavily disordered areas that have structures closer to enargite than to luzonite (Fig. 9).

All the crystals from which we obtained the SAED patterns and electron micrographs in Figures 7, 8, and 9 are free of Sb. All heavily disordered crystals, such as the one in the lower part of Figure 9, are Cu_3AsS_4.

Analyses of defects

Stacking defects in enargite can be interpreted as individual layers of luzonite and vice versa. In Figure 10a the matrix is a luzonite crystal that contains a three-layer twin; at the twin boundaries the ABA and CBC sequences result in (Cu+As+Sb)+S layers at the B positions that are in a hcp environment. Likewise, a single stacking fault in an enargite crystal (Fig. 10b) results in an ABC stacking sequence in which the (Cu+As+Sb)+S layer at the B position is in a local ccp environment.

Because enargite and famatinite having widely different Sb/As ratios can be intergrown, we hypothesize that such intergrowths can also occur on the scale of individual defects. If hcp and ccp layers have different compositions, the number of defects in a disordered crystal could determine the total composition; the disordered crystals could then be regarded as belonging to a polysomatic series that has Sb-free (or low-Sb) enargite and high-Sb famatinite as the two end-members. Similar polysomatic trends were suggested for biotite by Baronnet (1992).

To determine whether ccp layers in an enargite host are associated with higher Sb contents, we analyzed faults in two ways. (1) We looked for crystals in which defects occur in swarms next to defect-free areas; both defective and structurally perfect areas were analyzed. (2) Some Sb-bearing enargite crystals contain several-layer-thick ccp sequences; we analyzed such faults using the small (2 nm) electron beam produced by the field-emission gun of the CM200 microscope.

Both methods revealed that the compositions of defects and their surroundings are identical within analytical error (about ±3 mol% Cu_3SbS_4). An enargite crystal that contains a 13-layer luzonite lamella (Fig. 11) was aligned so

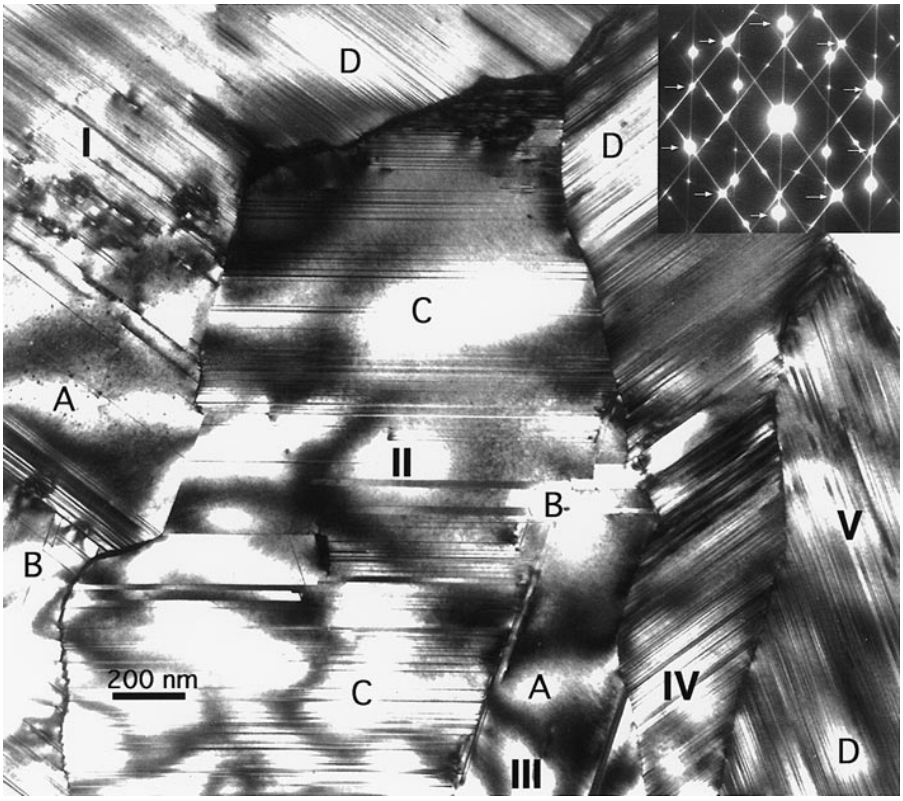

FIGURE 8. Low-magnification image of disordered luzonite crystals, viewed down [110]. The roman numerals mark five crystals that are related by integral multiples of 72° rotations around their common [110] zone axis, and the letters mark areas that have different degrees of disorder (see text). The SAED pattern was obtained from the entire area in the image.

that the electron beam was parallel to the plane of the fault. Three series of EDS spectra were collected across the fault; the size of the electron beam that was used in one of these series is shown by the white spots that are drawn at the positions where the analyses were done. The ratios of net X-ray counts within the Sb L-peak and the As K-peak vary slightly (between 0.10 and 0.19), but the variation is independent of the structural defect and remains within the analytical error, which in this case is estimated to be about ± 0.08. We obtained the same results in the other two series of analyses.

DISCUSSION

Our results suggest that coexisting enargite, luzonite, and famatinite are non-equilibrium assemblages that are metastably preserved, and thus the variations of ore-forming conditions may have been recorded in their microstructures and compositions. The wide variety of microstructures is in itself evidence for the persistence of metastable structures. Unlike other Cu sulfides (Pósfai and Buseck 1994), enargite and luzonite are stable in the electron beam and do not seem to change during sample preparation; ion-milled TEM specimens remained unchanged over a period of three years. The sharp chemical boundaries, as observed in zoned luzonite, indicate that there is no exchange of Sb and As across the interfaces; hence, we assume that no compositional changes occurred after the crystals formed and chemical interfaces reflect the variations of bulk fluid compositions during crystal growth.

Average structures and compositions

Individual structural defects in enargite and luzonite do not chemically differ from their host structures. Disordered areas or crystals with sizes larger than about 0.1 μm can be adequately characterized by a specific average structure and composition. Because the formation of atomic-scale structural features is not controlled by composition, it is meaningless to break down compositional data on the nanometer scale. Most compositional variations in enargite and luzonite could be observed at the resolution that is available with a scanning electron microscope (~1 μm). However, the true structural complexity can only be seen with HRTEM, and the average structures are best studied using SAED.

The compositions and average structures of about 35 enargite, luzonite, and famatinite crystals (or parts of crystals) are shown in Figure 12. In this ''structure-composition'' diagram the vertical axis tying luzonite and enargite represents structure and the horizontal axis represents composition. For example, a disordered crystal with 20% hcp and 80% ccp layers in its structure and with composition $Cu_3As_{0.6}Sb_{0.4}S_4$ would plot at point A. The hcp Cu_3SbS_4 phase in the upper right corner of the diagram is hypothetical; it is included here so that compositions outside the enargite-famatinite-luzonite triangle

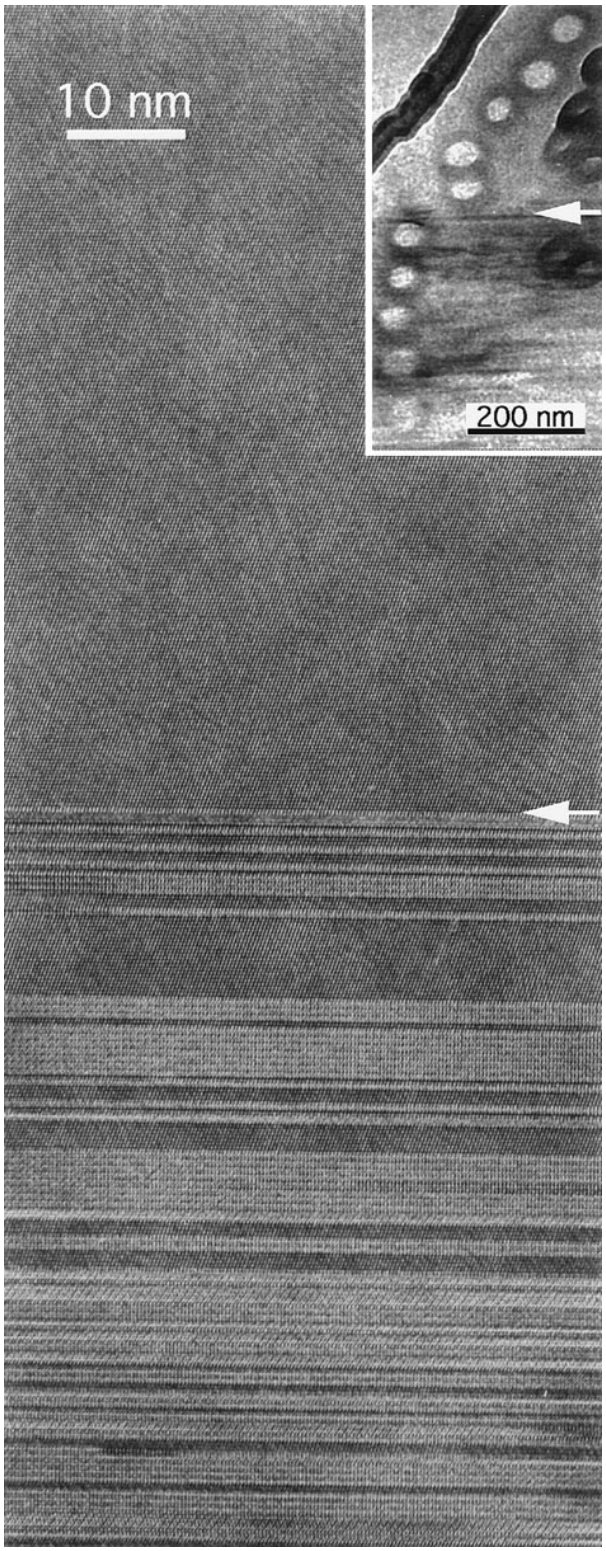

FIGURE 9. Intergrowth of ordered luzonite (above the white arrow) and heavily disordered enargite/luzonite. The inset shows the same area at lower magnification, with the contamination spots of earlier EDS analyses.

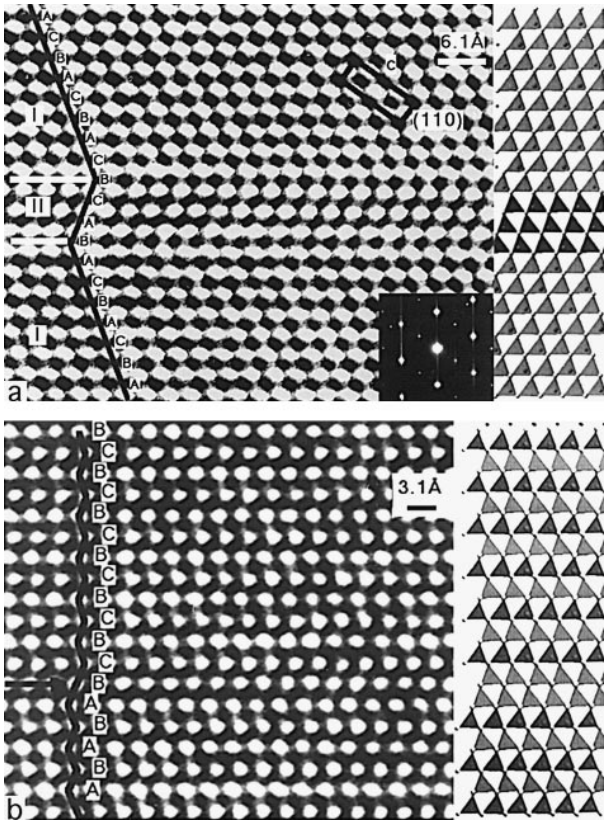

FIGURE 10. HRTEM images of individual defects in **a** luzonite and **b** enargite. The defects are marked by white lines in **a** and by the black arrow in **b**. I and II in **a** refer to two twin orientations. A, B, and C denote the stacking sequences of close-packed S layers; the white spots in the images correspond to S atom positions. (The white and black spots in **a** and **b** appear different because the two crystals do not have the same thickness.) The structure models on the right show the stacking of Cu, As, and Sb-filled tetrahedra at the scale of the HRTEM images.

could be plotted. Most average structures in Figure 12 were determined on the basis of HRTEM images, by counting hcp and ccp layers over areas containing hundreds of close-packed layers. For a few crystals the average structures were estimated (with an error of about ±5%) on the basis of the diffuse scattering in their SAED patterns; the diagram contains data points obtained from 113 analyses.

Several observations can be made by inspection of Figure 12. The central portion of the luzonite-enargite-famatinite triangle is empty, indicating that none of the Sb-containing crystals are strongly disordered. Compositions continuously range between 0 and 66% Cu_3SbS_4 in almost pure ccp crystals and hcp/ccp ratios continuously range between Sb-free enargite and luzonite. Defect-free, structurally 100% hcp enargite can contain as much Sb as slightly defective enargite. The most common types seem to be enargite crystals with 1 to 4% ccp layers and lu-

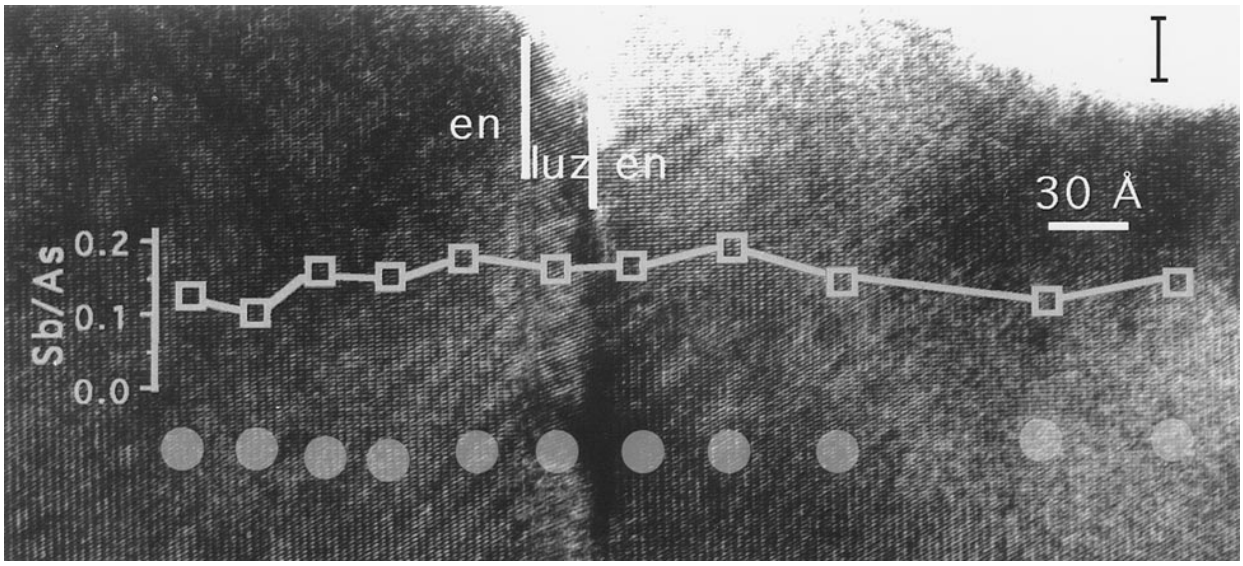

FIGURE 11. A 13-layer luzonite lamella in Sb-bearing enargite. The circles mark the positions of EDS analyses; the corresponding ratios of net X-ray counts for Sb and As are shown above them. The error bar is indicated in the upper right corner.

zonite crystals having about 1% hcp layers, regardless of their Sb contents.

The lack of an Sb-bearing, intermediate structure supports the existence of a miscibility gap (Fig. 1) between enargite and Sb-bearing luzonite-famatinite, as concluded by Skinner (1960) and Sugaki et al. (1982). The most Sb-rich enargite that coexists with luzonite-famatinite contains 11 mol% Cu_3SbS_4 (Fig. 4). Enargite with Cu_3SbS_4 contents greater than 11% occurs only in intergrowths with Mn-bearing tetrahedrite.

Effects of Sb fluctuations in the parent fluid

Enargite and famatinite are never in equilibrium with each other, as illustrated by the intervening field of luzonite (Fig. 1). We suggest that intergrowths between hcp and ccp structures (such as in Figs. 2, 3, and 4) form when compositional changes force a switch in the stacking sequence in which the close-packed layers are deposited. If this is correct, then in the case of the intergrowth shown in Figure 3, even the direction of crystal growth can be deduced. If the crystallization of luzonite preceded that of enargite in this crystal, then the structural change at the boundary between luzonite and the transition zone occurred without an apparent stimulus, since the transition zone has the same composition as luzonite. Alternatively, the growth of luzonite on preexisting enargite can be explained by an initial increase in the Sb content of the fluid (as reflected by the chemical boundary between enargite and the transition zone), forcing the structure to change to ccp (i.e., luzonite). The arrow shows the presumed direction of growth. The transition zone formed because the driving force of the structural change could be relatively small, as reflected by the small chemical difference between enargite and luzonite. If the compositional changes are large (Fig. 2), then no transitional structure forms and the direction of crystal growth cannot be established.

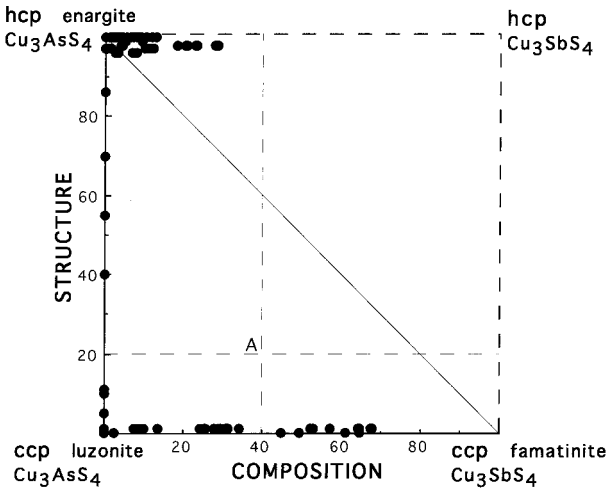

FIGURE 12. "Structure-composition" diagram showing 113 analyses obtained from 35 crystals. See text for explanation.

The zoned luzonite crystals and the data that plot on and slightly above the luzonite-famatinite axis in Figure 12 confirm the existence of a solid-solution series between luzonite and famatinite and also reflect the effects of fluctuations in the bulk Sb content of the ore-forming fluid. Both luzonite and enargite occur at the low-Sb end of the diagram. The formation of either the hcp or the ccp phase must be determined by temperature or compositional variations other than changes in the Sb/As ratio. Deviations from stoichiometric S/Zn ratios were shown to stabilize hcp wurtzite at temperatures where ccp sphal-

erite should be stable (Scott and Barnes 1972). As discussed above, small changes in the S/(Cu+As+Sb) ratios in enargite and luzonite are undetectable with the methods we used and so remain untested in our samples. However, microprobe analyses by Springer (1969) show a small and equal S excess over the stoichiometric value for luzonite and enargite; therefore, we think that variations in the S/(Cu+As+Sb) ratio are not important in the formation of either luzonite or enargite; instead, at low Sb contents the temperature presumably determines whether ccp or hcp crystals form.

Effects of thermal fluctuations

Crystals with average structures that plot along the line between enargite and luzonite in Figure 12 may be the results of thermal fluctuations. A large variety in the density and distribution of faults is shown in Figure 8; in some crystals faults and twinning along one set of close-packed (112)-type planes occur, whereas other grains contain intersecting faults and twins along two or three sets of cubic-close-packed planes. The common zone-axis orientation of the crystals could indicate that this assemblage formed by a solid-state transformation from a structure with higher symmetry; tennantite could be a possible parent phase. If the luzonite formed from tennantite, then the $(112)_{luz}$-type planes in the five crystals should correspond to the $(111)_{ten}$-type planes; however, there are five sets of $(112)_{luz}$-type planes in Figure 8 (as discussed in the Results section), whereas the maximum number of $(111)_{ten}$-type planes is only four. Similar heavily disordered structures were reported by Akizuki (1981) in ZnS that was heated to near the sphalerite→wurtzite transition temperature. From the information provided by Figures 7, 8, and 9, the most plausible explanation for the formation of heavily disordered, Sb-free enargite and luzonite is that such crystals formed near the transition temperature between luzonite and enargite. Their defects are probably growth features, and the common zone-axis orientations (as in Fig. 8) originate from the preferential nucleation of crystals on preexisting (112)-type planes.

The relative abundance of slightly faulted enargite and luzonite crystals (with 1 to 4% of their close-packed layers faulted in a random distribution) may indicate that the formation of a small number of defects is thermodynamically favored. Several theories have been proposed to explain certain degrees of stacking disorder in close-packed crystals; for a review, see Baronnet (1992).

A picture of temperature and Sb-content fluctuations emerges from Figure 12 and the above discussion. If our interpretation is correct that the enargite/famatinite interfaces and luzonite-famatinite zone boundaries are preserved just as formed, then they reflect bulk Sb-content variations in the ore-forming fluid. According to fluid-inclusion studies by Gatter (1991) on gangue minerals associated with the Recsk enargite, the temperature varied between about 300 °C and less than 150 °C. Our results in this study are consistent with the fluid-inclusion data and Figure 1. Intergrowths of Sb-rich enargite and tetrahedrite represent the highest temperature assemblages; in general, the occurrence of enargite indicates temperatures greater than about 280 °C (the transition point between luzonite and enargite), whereas Sb-free, ordered luzonite formed below 280 °C. The heavily disordered, Sb-free enargite/luzonite crystals could be useful as geological thermometers for they probably indicate temperatures near 280 °C.

The formation of a single defect is not individually controlled by composition or temperature; however, the combined effects of the actual temperature and fluid composition determine whether the structure of a crystal (or part of a crystal) will be ccp, hcp, or strongly disordered.

Acknowledgments

Reviews by Alain Baronnet and Peter Heaney improved the manuscript and are gratefully acknowledged. We thank István Dódony for discussions about defect structures and István Gatter for data on the genesis of the Recsk ore deposit. This study was supported by National Science Foundation grant EAR-9219376. We used TEMs located in the Center for High Resolution Electron Microscopy at Arizona State University.

References cited

Akizuki, M. (1981) Investigation of phase transition of natural ZnS minerals by high resolution electron microscopy. American Mineralogist, 66, 1006–1012.

Baronnet, A. (1992) Polytypism and stacking disorder. In Mineralogical Society of America Reviews in Mineralogy, 27, 231–288.

Barton, P.B., Jr. and Skinner, B.J. (1967) Sulfide mineral stabilities. In H.L. Barnes, Ed., Geochemistry of Hydrothermal Ore Deposits, p. 236–333. Holt, Rinehart and Winston, New York.

Basu (Sanyal), K., Bortnikov, N.S., Mookherjee, A., Mozgova, N.N., Sivtsov, A.V., Tsepin, A.I., and Vrublevskaja, Z.V. (1984) Rare minerals from Rajpura-Dariba, Rajasthan, India: V. The first recorded occurrence of a manganoan fahlore. Neues Jahrbuch für Mineralogie, Abhandlungen, 149, 105–112.

Buseck, P.R. and Self, P. (1992) Electron energy-loss spectroscopy (EELS) and electron channelling (ALCHEMI). In Mineralogical Society of America Reviews in Mineralogy, 27, 141–180.

Feiss, P.G. (1974) Reconnaissance of the tetrahedrite-tennantite/enargite-famatinite phase relations as a possible geothermometer. Economic Geology, 69, 383–390.

Fleischer, M. and Mandarino, J.A. (1995) Glossary of mineral species 1995 (7th edition), 280 p. The Mineralogical Record, Tucson.

Gaines, R.V. (1957) Luzonite, famatinite and some related minerals. American Mineralogist, 42, 766–779.

Gatter, I. (1991) Fluid inclusion studies on the Recsk ore complex (N-Hungary): II. The ore of Lahóca Old Mine. European Current Research on Fluid Inclusions, XI, Abstracts, 84–85.

Kanazawa, Y. (1984) Synthesis and lattice constants of luzonite-famatinite crystals. Bulletin of the Geological Survey of Japan, 35, 13–17.

Lévy, C. (1967) Énargite, stibioénargite, luzonite, stibioluzonite, famatinite. In Contribution à la Minéralogie des Sulfures de Cuivre du Type Cu_xXS_4, p. 101–124. B.R.G.M., Paris.

Luce, F.D., Tuttle, C.L., and Skinner, B.J. (1977) Studies of sulfosalts of copper: V. Phases and phase relations in the system Cu-Sb-As-S between 350° and 500 °C. Economic Geology, 72, 271–289.

Makovicky, E. and Karup-Møller, S. (1994) Exploratory studies on substitution of minor elements in synthetic tetrahedrite: I. Substitution by Fe, Zn, Co, Ni, Mn, Cr, V and Pb. Unit-cell parameter changes on substitution and the structural role of "Cu^{2+}". Neues Jahrbuch für Mineralogie, Abhandlungen, 167, 89–123.

Maske, S. and Skinner, B.J. (1971) Studies of the sulfosalts of copper: I. Phases and phase relations in the system Cu-As-S. Economic Geology, 66, 901–918.

Pósfai, M. and Buseck, P.R. (1994) Djurleite, digenite, and chalcocite: Intergrowths and transformations. American Mineralogist, 79, 308–315.

Pósfai, M. and Sundberg, M. (1998) Stacking disorder and polytypism in enargite and luzonite. American Mineralogist, 83, 365–372.

Scott, S.D. and Barnes, H.L. (1972) Sphalerite-wurtzite equilibria and stoichiometry. Geochimica et Cosmochimica Acta, 36, 1275–1295.

Skinner, B.J. (1960) Assemblage enargite-famatinite, a possible geothermometer. Geological Society of America Bulletin, 71, 1975.

Skinner, B.J., Luce, F.D., and Makovicky, E. (1972) Studies of the sulfosalts of copper: III. Phases and phase relations in the system Cu-Sb-S. Economic Geology, 67, 924–938.

Springer, G. (1969) Compositional variations in enargite and luzonite. Mineralium Deposita, 4, 72–74.

Sugaki, A., Kitakaze, A., and Shimizu, Y. (1982) Phase relations in the Cu_3AsS_4-Cu_3SbS_4 join. Science Reports of the Tohoku University 3rd Series, XV, 257–271.

Sugaki, A., Shima, H., and Kitakaze, A. (1976) Chemical compositions of enargite and luzonite-famatinite series minerals from the Kasuga and Akeshi mines, Kagoshima, Japan. Journal of the Mineralogical Society of Japan, 12, 206–213 (in Japanese) (not seen; extracted from Science Reports of the Tohoku University 3rd Series, XV, 257–271).

Manuscript received February 26, 1997
Manuscript accepted November 9, 1997